34th Annual International Conference of the IEEE EMBS
San Diego, California USA, 28 August - 1 September, 2012

Theoretical study of bone's microstructural effects on Rayleigh wave propagation

Maria G. Vavva, Leonidas N. Gergidis, Antonis Charalambopoulos, Vasilios C. Protopappas, *Member, IEEE*, Demosthenes Polyzos, Dimitrios I. Fotiadis, *Senior Member, IEEE*

***Abstract*— The linear theory of classical elasticity cannot effectively describe bone's mechanical behavior since only homogeneous media and local stresses are assumed. Additionally, it cannot predict the dispersive nature of Rayleigh wave which has been experimental observed. By adopting Mindlin Form II gradient elastic theory and performing Boundary Element (BEM) simulations we also recently demonstrated Rayleigh dispersion. In this work we use this theory to analytically determine the dispersion of Rayleigh wave. We assume an isotropic semi-infinite space with mechanical properties equal to those of bone and microstructure and microstructural effects. Calculations are performed for various combinations between the internal constants l_1, l_2, h_1, h_2 which corresponded to a) values from closed form relations derived from a realistic model and b) values close to the osteon's size. Comparisons are made with the corresponding computational results as well as with the classical elastic case. The agreement between the computational and the analytical results was perfect demonstrating the effectiveness of Mindlin's Form II gradient theory of elasticity to predict the dispersive nature of Rayleigh wave. This study could be regarded as a step towards the ultrasonic characterization of bone.**

I. Introduction

Ultrasonic wave propagation in cortical bone has been widely investigated using the classical elastic theory [1]. However, in non-homogeneous materials with microstructural effects like bone the stress state should be determined non-locally, which cannot be achieved using classical elasticity. Furthermore above 0.8 MHz (i.e., wavelength smaller than the cortical thickness) ultrasound propagates in bone as a dispersive surface Rayleigh wave rather than a dispersive guided wave, which cannot be also supported by classical elasticity. The dispersive nature of the guided and Rayleigh waves can be successfully described using Mindlin's Form II gradient theory of elasticity, which introduces intrinsic parameters that correlate microstructure with macrostructure [2]. By exploiting the simplest form of this theory (which incorporates two coefficients) we recently showed that the dispersion of the propagating guided waves is highly affected by bone's microstructure [3]. This was also in accordance with a subsequent computational study on guided wave propagation in 2D Boundary Element bone models with microstructural effects [4].

The dipolar gradient elastic theory has been used to explain Rayleigh wave dispersion phenomena that have been experimentally observed at high frequencies [5]. In two recent computational studies [6, 7] we also investigated the effect of bone's microstructure on Rayleigh wave propagation by adopting both the simple and the general Mindlin Form II gradient elastic theory (in which four constants are involved). Since the determination of the microstructural constants introduced in the stress analysis is an open issue when applying enhanced elastic theories to real problems, the constants were first assigned with values from closed form relations derived from a realistic model proposed by [4]. This model associates the internal length-scale values with the periodicity of geometrical and elastic properties of the osteons. Numerical simulations were also performed for different combinations between the internal constants with values at the order of the osteon's size [8]. By performing BEM simulations in cortical bone we confirmed that Rayleigh wave is dispersive only when the shear stiffness intrinsic parameter is different from the inertia one.

In this work we analytically determine the dispersion curve of Rayleigh wave in the context of Mindlin Form II gradient elasticity. Analytical solution is given for an isotropic semi-infinite space with microstructure and mechanical properties equal to those of bone. The values of the internal length scale parameters were in accordance with those examined in [7]. Comparisons are made with the corresponding computational results derived from [7] as well as with the analytical dispersion curve of the Rayleigh wave in the classical elastic case and were also compared to empirically selected values. In all cases, the analysis of the obtained signals is performed in the time-frequency (t-f) domain.

II. Materials and Methods

A. *Mindlin's Form II gradient elastic theory and Rayleigh wave dispersion*

In Mindlin's Form-II gradient elastic theory the potential

Manuscript received March 29, 2012.

M.G. Vavva and D.I. Fotiadis are in the Unit of Medical Technology and Intelligent Information Systems, Department of Material Science and Engineering, University of Ioannina, GR 45110, Ioannina, Greece (e-mails: mvavva@cc.uoi.gr, fotiadis@cc.uoi.gr).

L. N. Gergidis is with the Department of Material Science and Engineering, University of Ioannina, GR 45110, Ioannina, Greece (e-mail: lgergidi@uoi.gr).

A. Charalambopoulos is with the School of Applied Mathematical and Physical sciences, Department of Mathematics National Technical University of Athens, GR 15780, Athens, Greece (e-mail: acharala@math.ntua.gr).

V.C. Protopappas and D. Polyzos are with the Department of Mechanical Engineering and Aeronautics, University of Patras, GR 26500, Patras, Greece, (e-mails: vprotopappas@gmail.com, polyzos@mech.upatras.gr).

energy of an isotropic elastic body with microstructure of volume V is considered as a quadratic form of the strains and the gradient of strains [2]. The equation of motion in Mindlin Form-II for a homogeneous material with microstructural effects is given by:

$$(\lambda+2\mu)(1-l_1^2\nabla^2)\nabla\nabla\cdot\mathbf{u}-\mu(1-l_2^2\nabla^2)\nabla\times\nabla\times\mathbf{u} = \rho(\ddot{\mathbf{u}}-h_1^2\nabla\nabla\cdot\ddot{\mathbf{u}}+h_2^2\nabla\times\nabla\times\ddot{\mathbf{u}}), \quad (1)$$

where the operator ∇ is the Laplacian, $\mathbf{u}$ is the displacement vector and l_1, l_2, h_1, h_2 are intrinsic lengthscale parameters having units of length square (m^2) given by:

$$l_1^2 = 2(a_1+a_2+a_3+a_4+a_5)/(\lambda+2\mu), \quad (2)$$

$$l_2^2 = (a_3+2a_4+a_5)/2\mu, \quad (3)$$

$$h_1^2 = \frac{\rho' d^2\left[2\alpha^2+(\alpha+\beta)^2\right]}{3\rho}, \quad (4)$$

$$h_2^2 = \frac{\rho' d^2(1+\beta^2)}{3\rho}. \quad (5)$$

The parameters l_1, l_2 represent the effect of the stiffness of the elastic properties of the microstructure on the macrostructural behavior of the gradient elastic material whereas h_1, h_2 represent the effect of the inertia.

Considering the same density for microstructure and macrostructure, i.e., $\rho' = \rho$ and $\alpha_1 = \alpha_3 = \alpha_5 = 0$, $\alpha_2 = (\lambda/2)g^2$, $\alpha_4 = \mu g^2$ correspond to the simple or dipolar Mindlin's Form II gradient elastic theory.

Consider a semi infinite space and a Cartesian system Ox_1x_2 with the axis Ox_1 being the upper boundary. In the gradient theory the semi-infinite space is assumed free from stresses and double stresses i.e.

$$\mathbf{P}|_{x_2=0} = 0,\ \mathbf{R}|_{x_2=0} = 0, \quad (6)$$

where $\mathbf{P}$ and $\mathbf{R}$ are the traction vector and the double traction vector respectively. Solution to (1) and satisfaction of the boundary conditions result in a system of four unknown constants. The components of the determinant of the system are given in the Appendix. Vanishing of the determinant yields the characteristic dispersion equation of the Rayleigh wave propagating in a semi-infinite gradient elastic space.

B. Computation of Rayleigh wave

The semi-infinite space was assumed to have mechanical properties equal to those of bone i.e., Young's modulus E_{bone} = 14 GPa, Poisson's ratio ν_{bone} = 0.37 and density ρ = 1500 Kg/m^3 [1,10]. Four different cases of the intrinsic parameters were investigated. Case1 corresponds to values derived from Ben-Amoz model [4], i.e., $l_1 = l_2 = h_1 = 1.04\times10^{-4}m$ and $h_2 = 0.74\times10^{-4}m$. The next three cases correspond to different combinations between the internal constants, i.e., $l_1 = h_1 = 1.04\times10^{-4}m$, $l_2 = h_2 = 0.74\times10^{-4}m$ in Case2, $l_1 = l_2 = h_2 = 0.74\times10^{-4}m$, $h_1 = 1.04\times10^{-4}m$, in Case3 and $l_1 = h_1 = h_2 = 0.74\times10^{-4}m$ $l_2 = 1.04\times10^{-4}m$, in Case4.

C. Numerical solution

Numerical solution to the problem was given using a symbolic algebra software (Mathematica, Wolfram Research Inc., IL, USA). The frequency step equals to 10 Krad/sec since no differences were observed in the results for smaller steps [3].

III. Results

The Rayleigh wave calculated for all the examined cases is presented in Fig. in the form of frequency-group (f, c_g) velocity dispersion curves (dashed lines). The corresponding analytical group velocity dispersion curve in the classical elastic case derived from the frequency equation for surface waves [9] is also presented in Fig.1 (dotted line) for comparison purposes.

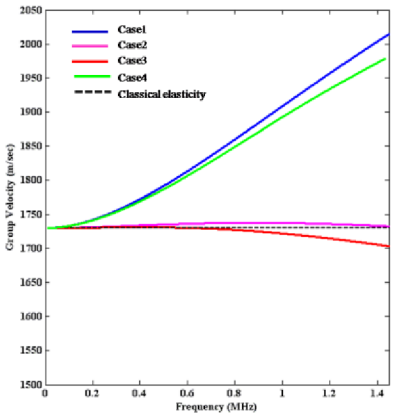

Figure 1. Group velocity dispersion of the Rayleigh wave analytically derived for Case1,2,3 and 4. The classical elastic case is also presented (dotted line).

It can be seen that in Case1 (i.e., derived from Ben Amoz model [4]) is strongly dispersive with its velocity to be highly modified from that in the classical elastic case. In Case2 the Rayleigh velocity is almost identical to that in the classical case, exhibiting thus no dispersion. In Case3 the Rayleigh velocity is slightly lower than the classical case as the frequency increases (i.e., at 1.45MHz it is 27m/sec lower). Finally in Case4 the velocity of the Rayleigh takes higher values in the classical cases as the frequency increases exhibiting dispersion.

To compare the analytical curves with the computational ones [7], for transmitter-receiver distance 60*mm* i.e., equal to that used in [7] the curves of the Rayleigh wave derived from both gradient and classical elasticity were converted to t-f curves and were superimposed on the t-f plane of the corresponding signals obtained from the BEM models [7]. T-f signal analysis has been typically used by our group for the detection of the guided modes propagating in intact and healing bones [1]. The reassigned Smooth-Pseudo Wigner-Ville (RSPWV) energy distribution function has been also used in [7] since it accurately localizes guided waves.

The t-f diagrams of the Rayleigh wave for Cases1, 2, 3 and 4 are shown in Figs. 2, and Figs 3a, b and c respectively. The computational Rayleigh signal is depicted with the black line, whereas the corresponding analytical curves in the gradient and the classical elastic case are depicted with the blue dashed line and the magenta dotted line respectively.

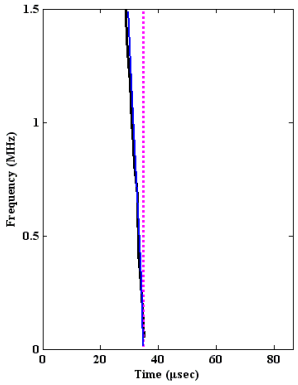

Figure 2. T-f representation of Rayleigh wave dispersion for Case1 ($l_1 = l_2 = h_1 = 1.04\times10^{-4} m$, $h_2 = 0.74\times10^{-4} m$).

In Case1, the computational Rayleigh dispersion can be perfectly characterized by the corresponding analytical curve calculated for the gradient elastic case (Fig.2). In Cases2 and 3 the analytically derived arrival times of the Rayleigh wave in the gradient and classical elasticity are almost identical. Therefore slight differences (from the classical case) in the group velocity, mainly in Case3 (Fig.1), become rather practically insignificant in the t-f plane since the difference in the arrival time is very small. The computational Rayleigh wave is also well characterized by the analytical curves in both Cases2 and 3 in the 0-1.43MHz frequency range. In higher frequencies the computational t-f curve is slightly deviated from the theoretical ones. For instance at 1.467MHz the difference between the computational and analytical arrival time is 1.51μsec in both Cases. Finally in Case4 the Rayleigh dispersion obtained from a BEM model can be perfectly described from the corresponding analytical gradient elastic t-f curve.

IV. Discussion

In this study we analytically calculated for the first time the dispersion curve of the Rayleigh wave propagating in semi-infinite media with microstructure and properties equal to those of bone. Microstructural effects were accounted by using Mindlin's Form II gradient elastic theory. Although several enhanced theories have been proposed for the investigation of microstructural effects in bones [3], Mindlin's gradient elastic theory has become attractive because of its simplicity and the symmetry of all stress tensors involved.

Since no conclusion has been drawn regarding the values of the microstructural constants, we first determined them using closed form relations derived from a realistic model [4] with the representing volume element based on the osteon's characteristics. Three additional combinations between the microstructural parameters were also examined. In all cases the values were similar to those presented in our previous computational study [7] so as to perform direct comparisons between the analytical and computational results.

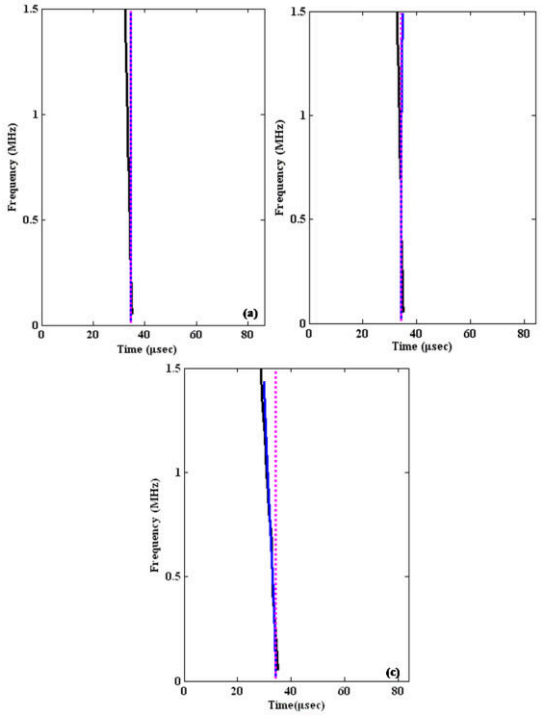

Figure 3. T-f representation of Rayleigh wave dispersion for (a) Case2, (b) Case3 and (c) Case4.

In Case1 (i.e., $l_1 = l_2 = h_1 \neq h_2$) and Case4 (i.e., $l_1 = h_1 = h_2 \neq l_2$) the Rayleigh velocity was significantly modified from that in the classical elastic case as the frequency increases, exhibiting dispersion. In Case2 (i.e., $l_1 = h_1$, $l_2 = h_2$) was almost identical to that in the classical case. In Case3 (i.e., $l_1 = l_2 = h_2 \neq h_1$) the velocity of the Rayleigh wave was anticipated non-dispersive but some slight dispersion is observed. However in the t-f plane (Fig. 4) this could not be observed which suggests that Rayleigh wave arrives simultaneously without exhibiting dispersion.

Our findings demonstrate that dispersion of Rayleigh waves occurs when $l_2 \neq h_2$ i.e., when microstructural effects are represented by different stiffness and inertia length scale parameters no matter which are the values of h_1, l_1 . This is in agreement with our previous findings in [7]. Nevertheless, in that study the computational results were validated by observing the asymptotic behavior the first order modes derived from the dipolar gradient elastic theory. To this end, the analytical Rayleigh curves for all cases were superimposed in the corresponding t-f diagrams of the signals from [7]. When $l_2 \neq h_2$, the numerical simulations were in perfect agreement with the analytical solutions from gradient elasticity. When $l_2 = h_2$,a very small deviation was observed only at frequencies higher than 1.43MHz. However, these deviations could be possibly attributed to computational problems.

V. CONCLUSION

We presented an analytical study on the effect of mictrostructure on Rayleigh wave propagation by using the Mindlin Form II gradient elastic theory. Calculations were performed for various combinations between the microstructural constants and the results were compared with the corresponding computational signals obtained from [7]. Overall our findings demonstrate the dispersive nature of the Rayleigh wave under certain conditions, i.e., only when the shear stiffness constant is different from the inertia internal one. (i.e. $l_2 \neq h_2$). In addition the analytical results were in good agreement accordance with the computational ones. Overall Mindlin's Form II gradient elastic theory is more efficient in predicting the dispersive nature of Rayleigh wave and thus it could be proved useful in providing more precise interpretations of clinical measurements in real bones.

APPENDIX

The components of the determinant of the system are:

$$A_{11} = -2ikp\mu - (ik^3 p + ikp^3)(a_1 + 2a_2) + \frac{1}{2}(ik^3 p - ikp^3)(-a_1 - a_3)$$
$$+ ikp\rho\omega^2(2h_2^2 - \frac{d^2\rho'}{3\rho}) - \frac{3}{2}ik^3 pa_3 + \frac{3}{2}ikp^3 a_3 - 4ik^3 pa_4$$
$$- ikp^3(-a_4 - \frac{3a_5}{2}) - ikp^3(-a_4 - \frac{a_5}{2}) - 4ik^3 pa_5$$

$$A_{12} = -2ik\mu r_p - ik^3 a_1 r_p - 2ik^3 a_2 r_p + \frac{1}{2}ik^3(-a_1 - a_3)r_p - \frac{3}{2}ik^3 a_3 r_p$$
$$- 4ik^3 a_4 r_p - 4ik^3 a_5 r_p + ika_1 r_p^3 + 2ika_2 r_p^3 - \frac{1}{2}ik(-a_1 - a_3)r_p^3 +$$
$$\frac{3}{2}ika_3 r_p^3 - ik(-a_4 - \frac{3a_5}{2})r_p^3 - ik(-a_4 - \frac{a_5}{2})r_p^3 + ik\rho\omega^2 r_p(2h_2^2 - \frac{d^2\rho'}{3\rho})$$

$$A_{13} = k^2\mu + q^2\mu + \frac{k^4 a_1}{2} - \frac{1}{2}k^2 q^2 a_1 + \frac{k^4 a_3}{2} - \frac{q^4 a_3}{2} + k^4 a_4 + 3k^2 q^2 a_4$$
$$+ k^2 q^2(-a_4 - \frac{3a_5}{2}) + q^4(-a_4 - \frac{a_5}{2}) + \frac{3k^4 a_5}{2} + \frac{5}{2}k^2 q^2 a_5$$
$$- k^2\rho\omega^2(h_2^2 - \frac{d^2\rho'}{3\rho}) + q^2\rho\omega^2(h_2^2 - \frac{d^2\rho'}{3\rho}) - q^2\rho\omega^2(2h_2^2 - \frac{d^2\rho'}{3\rho})$$

$$A_{14} = k^2\mu + \frac{k^4 a_1}{2} + \frac{k^4 a_3}{2} + k^4 a_4 + \frac{3k^4 a_5}{2} + \mu r_s^2 - \frac{1}{2}k^2 a_1 r_s^2 + 3k^2 a_4 r_s^2$$
$$- \rho\omega^2 r_s^2 h_2^2 + k^2(-a_4 - \frac{3a_5}{2})r_s^2 + \frac{5}{2}k^2 a_5 r_s^2 - \frac{1}{2}a_3 r_s^4 + (-a_4 - \frac{a_5}{2})r_s^4 -$$
$$k^2\rho\omega^2(h_2^2 - \frac{d^2\rho'}{3\rho})$$

$$A_{21} = -k^2\lambda + p^2\lambda + 2p^2\mu - \frac{3k^4 a_1}{2} + \frac{3}{2}k^2 p^2 a_1 - 2k^4 a_2 + 2k^2 p^2 a_2 +$$
$$p^4(-a_1 - a_3) + p^4(-a_1 - 2a_2 - \frac{a_3}{2}) + k^2 p^2(a_1 + 2a_2 + \frac{a_3}{2}) - k^4 a_3 +$$
$$\frac{3}{2}k^2 p^2 a_3 - \frac{p^4 a_3}{2} + k^2 p^2(a_1 + a_3) + 4k^2 p^2 a_4 + p^4(-a_4 - \frac{3a_5}{2}) +$$
$$p^4(-a_4 - \frac{a_5}{2}) + 2k^2 p^2 a_5$$

$$A_{22} = -k^2\lambda - \frac{3k^4 a_1}{2} - 2k^4 a_2 - k^4 a_3 + \lambda r_p^2 + 2\mu r_p^2 + \frac{3}{2}k^2 a_1 r_p^2$$
$$k^2(a_1 + 2a_2 + \frac{a_3}{2})r_p^2 + k^2(a_1 + a_3)r_p^2 + 4k^2 a_4 r_p^2 + 2k^2 a_5 r_p^2$$
$$+ (-a_1 - 2a_2 - \frac{a_3}{2})r_p^4 + (-a_4 - \frac{3a_5}{2})r_p^4 - \rho\omega^2 r_p^2(h_1^2 - h_2^2 + \frac{d^2\rho'}{3\rho}) +$$
$$(-a_4 - \frac{a_5}{2})r_p^4 - \rho\omega^2 r_p^2(2h_2^2 - \frac{d^2\rho'}{3\rho}) + k^2\rho\omega^2(h_1^2 - h_2^2 + \frac{d^2\rho'}{3\rho}) +$$
$$+ 2k^2 a_2 r_p^2 + \frac{3}{2}k^2 a_3 r_p^2 + (-a_1 - a_3)r_p^4 - \frac{1}{2}a_3 r_p^4$$

$$A_{23} = 2ikq\mu + \frac{1}{2}ik^3 qa_3 - \frac{1}{2}ikq^3 a_3 + \frac{5}{2}ik^3 qa_5 + 3ik^3 qa_4 + ikq^3 a_4$$
$$+ ikq^3(-a_4 - \frac{3a_5}{2}) + ikq^3(-a_4 - \frac{a_5}{2}) + \frac{3}{2}ikq^3 a_5 - ikq\rho\omega^2(2h_2^2 - \frac{d^2\rho'}{3\rho})$$

$$A_{24} = 2ik\mu r_s - \frac{1}{2}ik^3 a_1 r_s - \frac{1}{2}(ik^3 - ikr_s^3)(-a_1 - a_3) + 3ik^3 a_4 r_s + \frac{5}{2}ik^3 a_5 r_s + \frac{1}{2}ika_1 r_s^3$$
$$+ ika_4 r_s^3 + ik(-a_4 - \frac{3a_5}{2})r_s^3 + ik(-a_4 - \frac{a_5}{2})r_s^3 + \frac{3}{2}ika_5 r_s^3 - ik\rho\omega^2 r_s(2h_2^2 - \frac{d^2\rho'}{3\rho})$$

$$A_{31} = -\frac{1}{2}a_3(ik^3 - ikp^2) - \frac{1}{2}(ik^3 - ikp^2)(a_1 + a_3) + ikp^2(a_4 + \frac{a_5}{2}) + ikp^2(a_4 + \frac{3a_5}{2})$$

$$A_{32} = -\frac{1}{2}ik^3(a_1 + 2a_3) + \frac{1}{2}ikr_p^2(a_1 + 2a_3) + ik(a_4 + \frac{a_5}{2})r_p^2 + ik(a_4 + \frac{3a_5}{2})r_p^2$$

$$A_{33} = \frac{1}{2}k^2 qa_3 - \frac{q^3 a_3}{2} + k^2 q(-a_4 - \frac{3a_5}{2}) + q^3 + (-a_4 - \frac{a_5}{2})$$

$$A_{34} = \frac{1}{2}k^2 a_3 r_s + k^2(-a_4 - \frac{3a_5}{2})r_s - \frac{1}{2}a_3 r_s^3 + (-a_4 - \frac{a_5}{2})r_s^3$$

$$A_{41} = p^3(-a_1 - a_3) + p^3(-a_1 - 2a_2 - \frac{a_3}{2}) + k^2 p(a_1 + 2a_2 + \frac{a_3}{2}) +$$
$$\frac{1}{2}k^2 pa_3 - \frac{p^3 a_3}{2} + k^2 p(a_1 + a_3) + p^3(-a_4 - \frac{3a_5}{2}) + p^3(-a_4 - \frac{a_5}{2})$$

$$A_{42} = k^2(a_1 + 2a_2 + \frac{a_3}{2})r_p + \frac{1}{2}k^2 a_3 r_p + k^2(a_1 + a_3)r_p + (-a_1 - a_3)r_p^3$$
$$+ (-a_1 - 2a_2 - \frac{a_3}{2})r_p^3 - \frac{1}{2}a_3 r_p^3 + (-a_4 - \frac{3a_5}{2})r_p^3 + (-a_4 - \frac{a_5}{2})r_p^3$$

$$A_{43} = \frac{1}{2}(ik^3 - ikq^2)(a_1 + 2a_3) - ikq^2(a_4 + \frac{a_5}{2}) - ikq^2(a_4 + \frac{3a_5}{2})$$

$$A_{44} = \frac{1}{2}ik^3(a_1 + 2a_3) - \frac{1}{2}ikr_s^2(a_1 + 2a_3) - ik(a_4 + \frac{a_5}{2})r_s^2 - ik(a_4 + \frac{3a_5}{2})r_s^2.$$

REFERENCES

[1] V.C. Protopappas, M.G. Vavva, D.I. Fotiadis K.N. Malizos,"Ultrasonic Monitoring of Bone Fracture Healing", IEEE Trans. on *Ultr. Ferroel. Freq. Contr.*, vol. 55 (6), 1243-1254, 2008

[2] R.D. Mindlin, "Micro-structure in linear elasticity," Arch. Rat. Mech. Anal., vol. 16, pp. 51-78, 1964.

[3] M.G. Vavva, V.C. Protopappas, L.N.Gergidis, A. Charalambopoulos, D.I. Fotiadis, and D. Polyzos, "Velocity dispersion Curves of Guided Waves Propagating in a Free Gradient Elastic Plate: Application to Cortical Bone," *Journ. Acoust. Soc. Amer.* vol. 125, pp. 3414-3427, 2009.

[4] M. Ben-Amoz, "A dynamic theory for composite materials," *Journ.* Appl. Math. Phys. vol. 27, pp. 83-99, 1976.

[5] H. G. Georgiadis, I. Vardoulakis, and E.G. Velgaki, "Dispersive Rayleigh-wave propagation in microstructured solids characterized by dipolar gradient elasticity," *J. Elasticity*, vol. 74, pp. 17-45, 2004.

[6] M.G. Vavva, A. Papacharalampopoulos, V.C. Protopappas, D.I. Fotiadis, and D. Polyzos, "BEM Simulations of Rayleigh Wave Propagation in Media with Microstructural Effects: Application to Long Bones," *in proc. of 32nd Intern. Conf. of IEEE Eng. in Med. and Biol. Soc.*, August 2010.

[7] M.G. Vavva, V.C. Protopappas, D.I. Fotiadis, and D. Polyzos, "A numerical study on the propagation of Rayleigh and guided waves in cortical bone according to Mindlin's Form II gradient elastic theory," *Journ. Acoust. Soc. Amer.* vol. 130, pp. 1060-1070, 2011.

[8] J.Y. Rho, "Mechanical properties and the hierarchical structure of bone" Med. Eng. Phys., vol. 20 (2), pp. 92-102, 1998.

[9] Graff, F. K., Wave Motion in Elastic Solids (Oxford University Press, Oxford, 1975).

[10] A. R. Najafi, A. Arshi, M. Eslami, S. Fariborz, and M. Moeinzadeh, "Micromechanics fracture in osteonal cortical bone: A study of the interactions between microcrack propagation, microstructure and the material properties", *J. of Biomechanics* 40, pp. 2789, 2007.